Indian Journal of Engineering & Materials Sciences
Vol. 29, October 2022, pp. 605-614
DOI: 10.56042/ijems.v29i5.50542

Assessment of Intermittent Leather based on Image Score Pattern

S Nithiyanantha Vasagam[a*], & M Sornam[b]

[a]Knowledge Portfolio Management Division, CSIR-Central Leather Research Institute, Adyar, Chennai 600 020, India

[b]Department of Computer Science, University of Madras, Guindy Campus, Chennai 600 025, India

Received: 29 May 2021; Accepted: 8 October 2021

The process of intermittent leather inspection is being predominantly carried out with the support of human intervention based on homogenous distribution of colors. However, results of the observations between one experts to another expert may be different in opinion. Therefore, to emphasis some sort of supporting hand to the experts while taking decision, the authors have introduced an algorithm based on Image Score Pattern to distinguish between defect versus non-defect intermittent leather images. About 32 features generated from Gray Level Co-occurrence Matrix, Simple Linear Iterative Clustering and Minimum Spanning Tree Clustering from the training and testing datasets of about 1132 and 404 generated. The results of the classifier Support Vector Machine has confirmed the accuracy of 84% for the proposed Image Score Pattern method for these datasets. Similarly, other performance measures such as Precision, Recall, F1-Score, Specificity and Error Rate are also confirming that proposed method is performing in aligning of intermittent leather.

Keywords: Intermittent Leather, Image Score Pattern, Gray Level Co-occurrence Matrix, Simple Linear Iterative Clustering, Support Vector Machine

1 Introduction

The world trade of leather industry is about USD 253 Billion as per the exporters value accounted for raw hides & skins, finished leather, goods & garments, saddlery & harness, and Footwear. Hides and skins from bovine (including cattle and domestic buffalo), sheep, goat and pig are the basic raw materials for the leather industry in which bovine hides & skins is accounted for 65% and annually a total of about 1.7 Billion sq. m. of finished leathers are produced world over from these materials[1].

The processing of Raw Hides & Skins are needs to process at various stages to convert into a useful product, which is finished leather. Leather industry is a by-product industry[2] could have variations with reference to the quality due to origin and animal rearing practise. Accordingly, Trade value is arrived by categorizing the processed leather based on homogeneity, this process referred as assortment or leather inspection. The quality assurance is the key factor that decide the economy of the industry that is consistent and objective in nature.

At present, Assortment of leather in tanning sector processed predominantly by the intervention of human experts based on visual observation on surface defects[3]. This process of categorising is a labour intensive and time-consuming activity; at the same time the rejection rate is a big concern. This gives an opportunity to the authors to extend with a support system to the experts.

Classification on wet blue leather was adopted by Poelzleitner, W *et al.*[4] using hierarchical approach to recognise the error rate during evaluation of defects which are difficult to observed by human inspector's while detecting quality on leather surfaces.

Lidiya Georgieva *et al.*[5] has suggested the amount of usable area in wet blue hides and adopted statistical analysis of the distribution of gray levels through histogram. They have evaluated Chi Square (χ^2) test to count the pixels using standard histogram to understand the quality determination of leather surfaces on color distribution in identification of surface leather defects. The M is a standard histogram and N is a studied histogram and to compare the relationship between M and N as given in Eq. (1).

$$\chi^2 = \sum_{p=0}^{q} \left(\frac{(Mp-Np)^2}{Mp+Np} \right) \quad \ldots (1)$$

Roberto Viana *et al.*[6] has adopted the stochastic algorithm for estimation of parameters using simulated annealing. The features like entropy, contrast, angular second moment, inverse difference

* Corresponding author (E-mail: nvasagam@clri.res.in)

moment, energy and homogeneity of Gray Level Co-occurance Martices (GLCM) are extracted for calculation over the raw hide. The comparison of classifiers, Support vector machines using sequential minimal algorithm (SMO) and library LIBSVM, the algorithms of Boost IBJK, BoostJ48 and Multilayer Perceptron (MLP) are examined through confusion matrix to understand the accuracy of metrics of Recall, Precision & accuracy. The authors observed that the performance of LIBSVM is better than other classifiers.

Patricio Villar, *et al*.[7] has proposed an automatic method for defect classification on wet blue leather based on the Sequential Forward Selection Method from the feature extracted for classification from First Order Statistics, Contrast Characteristics, Haralick descriptors, Fourier & Cosine Transform, Hu moments with information about intensity, Local binary Patterns and Gabor Features with an accuracy of 95%. Shivashankar S *et al*.[8] has proposed a histogram based feature extraction based on intensity of color and followed by classification using K-Nearest Neighbour (K-NN) method with an accuracy of 89.47% from the features mean, standard deviation, homogeneity, slope and entropy.

Binary Classification on wet blue and raw hide stage in goat leather was carried out by R.F. Periera *et al*.[9] using machine learning on custom based dataset has been used by with 1874 images. Using Artificial Neural Network, Jawahar, M *et al*.[10] reported defect detection using multi-level thresholding algorithm with a classification accuracy of 88.6% to segment defective and non-defective regions of leather on custom based dataset consisting of 90 leather images comprising 20 good leather and 50 defective samples. Sze-Teng Lion, *et. al.*[11] has proposed an automatic defect identification system to segment irregular regions on a custom based dataset calf leather consisting of 584 images, which were trained and tested using by deep learning model. The evaluation metrics of specificity, precision, F1-Score, error rate and accuracy were worked-out and it was observed that the accuracy of segmentation for the training data is 91.5% and for the testing data is 70.35%.

Based on the above literature survey, there is an ample scope to introduce a support system in aligning of intermittent leather images based on the non-homogeneous color distribution. The summary of contribution of this article is follows:

- Pre-processing of the image using Gaussian filter, Laplacian Operator, Gaussian filter following with Laplacian Operator, Laplacian Operator following with Gaussian filter and generation of four image datasets namely DGF, DLO, DGFLO and DLOGF.
- Key Feature has identified from the above said four datasets consisting of the features such as Contrast, Dissimilarity, Homogeneity, Energy, Correlation and Angular Second Moment from Gray Level Co-occurrence Matrix (GLCM).
- Additionally, two more key features are also created with Threshold Value, which is extracted from Simple Linear Iterative Clustering (SLIC) and Minimum Spanning Tree Clustering (MSTC) from the above said four datasets.
- Class labels such as GL, SL and M are outcomes from the four datasets using the key feature.
- The authors have proposed a new algorithm for construction of Image Score Pattern (ISP) using python code for the dataset to separate the defect versus non-defect leather images.
- Performance measures such as Accuracy, Error Rate, Recall, False Positive Rate, Specificity, Precision and Prevalence are also explored in calculating the outputs of class labels.

Accordingly, the authors proposing the main objective of this study is to classify the intermittent leather for post tanning process with the proposed approach by which of extending a support hand to the leather assorter.

The structure of this remaining research article would consist of Material & Approach in which collection of dataset, pre-processing, feature extraction, feature selection, and Classification discussed.

2 Materials and Methods

The images of about 384 intermittent leathers have taken for this study. Following to which training and testing feature values are generated in a csv file format. The study is carried out in four steps namely as indicated in Fig. 1.

- Collection of Intermittent leather images,
- Pre-processing, dataset Generation and Feature Extraction,
- Feature Selection & Classification, and
- Results and Discussion.

2.1 Collection of Intermittent leather images

Collection of image dataset is a critical part for this study, since non-existence of dataset for leather defects

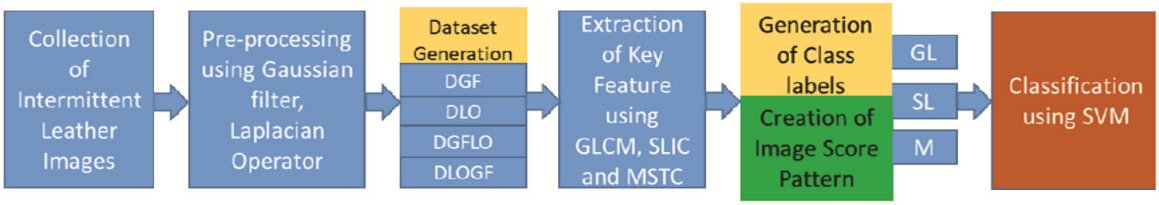

Fig. 1 — Process Flow.

having non-homogenous[12]. However, Amorim, W.P., *et al.*[13] has brought a custom based Nelore and Here for Tannery, Brazil dataset consisting of 2000 number of images but is not available in public domain. Accordingly, in this proposed study, a custom based training and testing dataset used for classification of intermittent leather images based on features extracted from GLCM about 241 and 143 respectively of which 283 is defect leather and 101 is non-defective leather. The images are originally taken from Konica camera and afterwards for the study the images were cropped in the size of 300 * 300 in 24-bit depth with horizontal and vertical resolution in 96 dpi.

2.2 Pre-processing, Dataset Generation and Feature Extraction

In digital image processing (Baxes *et al.* & Ekstrom *et al.*)[14-15], texture symbolizes (Yang *et al*,)[16] the detail of the surface on pixel basis. The analysis of texture of an image is based on spatial difference of color (Wang and Bu *et al.*)[17]. In addition to this, on the basis of size and shape the texture details are observed. To smooth the image for better clarity without noise (Sivakumar *et al.* & Hsu and Wu *et al.*)[18-19], Gaussian filter (Basu *et al.* 2002)[20] has been explored. It reduces the contrast while filtering in linear as shown Eq. (2).

$$g(x)=\sqrt{(a/\pi)}e^{(-ax^2)} \quad \ldots (2)$$

Canny edge detection (Bao *et al.*)[21] is a technique that has ability to identify all real edges. It extracts useful structural information from different vision objects and significantly reduce the amount of data to be processed as derivative which is shown in Eq. (3).

$$L(o) = \blacktriangledown(G*I) \quad \ldots (3)$$

where G is Gaussian and I is the image and it is an another derivative operator to find the edges in an image is Laplacian Operator (Wang *et al.*)[22]. It operates in the direction of inward and outward edges while classifying. Feature of an image has to be extracted in Image processing to analysis the surface color.

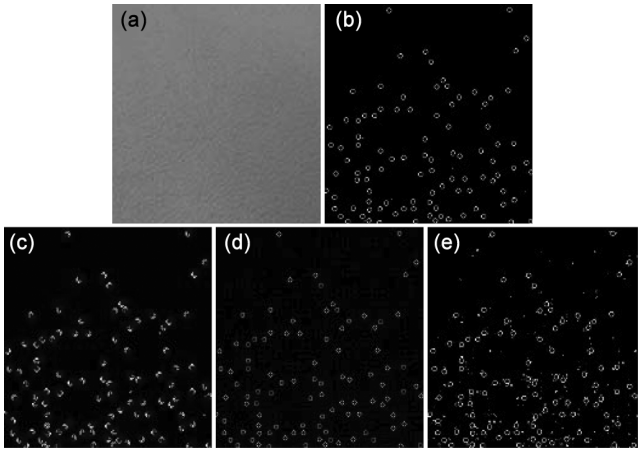

Fig. 2 — (a) Sample No 3 of actual intermittent leather, (b) Sample No 3 of actual intermittent leather with Gaussian filter, (c) Sample No 3 of actual intermittent leather with Laplacian Operator, (d) Sample No 3 of actual intermittent leather with Gaussian filter following with Laplacian Operator, and (e) Sample No 3 of actual intermittent leather with Laplacian Operator following with Gaussian filter.

The data of the image is enhancing during the pre-processing with the removal of unwanted distortion's (Taneja *et al.*)[23]. To smooth the image for better clarity without noise (Patel and Gamit *et al.*)[24], Gaussian filter has been explored using canny edge detection and also employed to Laplacian Operator to find the edges in images. Initially, the authors have generated two image datasets namely Dataset consisting of images with Gaussian filter (DGF), Dataset consisting of images with Laplacian Operator (DLO). Further, the authors have implemented hybrid based approach to generate another two Dataset by combining together Gaussian filter Laplacian Operator they are consisting of images with Gaussian filter following with Laplacian Operator (DGFLO) and Dataset consisting of images with Laplacian Operator following with Gaussian filter (DLOGF). A sample of intermittent leather images of consisting of 3, 17, 29, 84, 189, 240, 267 & 283 and its corresponding various image datasets are shown in Figs 3-9.

The GLCM technique is a way of extracting features such as second order statistical texture

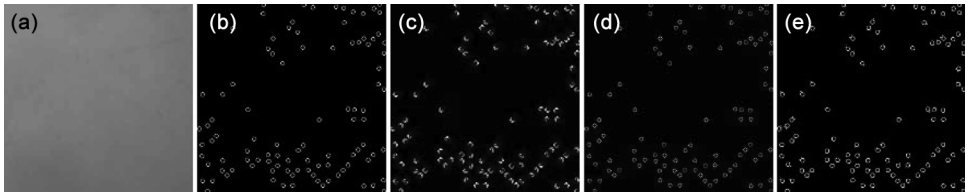

Fig. 3 — (a) Sample No 17 of actual intermittent leather, (b) Sample No 17 of actual intermittent leather with Gaussian filter, (c) Sample No 17 of actual intermittent leather with Laplacian Operator, (d) Sample No 17 of actual intermittent leather with Gaussian filter following with Laplacian Operator, and (e) Sample No 17 of actual intermittent leather with Laplacian Operator following with Gaussian filter.

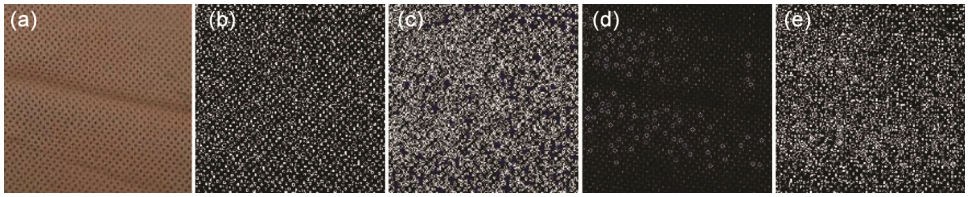

Fig. 4 — (a) Sample No 29 of actual intermittent leather, (b) Sample No 29 of actual intermittent leather with Gaussian filter, (c) Sample No 29 of actual intermittent leather with Laplacian Operator, (d) Sample No 29 of actual intermittent leather with Gaussian filter following with Laplacian Operator, and (e) Sample No 29 of actual intermittent leather with Laplacian Operator following with Gaussian filter.

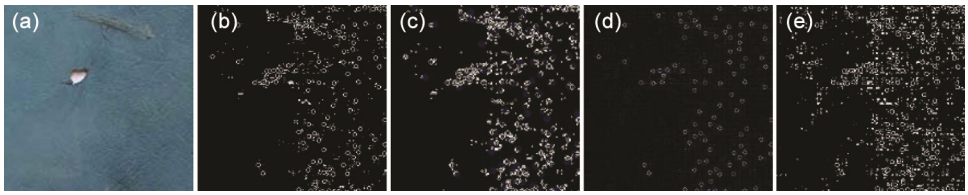

Fig. 5 — (a) Sample No 84 of actual intermittent leather, (b) Sample No 84 of actual intermittent leather with Gaussian filter, (c) Sample No 84 of actual intermittent leather with Laplacian Operator, (d) Sample No 84 of actual intermittent leather with Gaussian filter following with Laplacian Operator, and (e) Sample No 84 of actual intermittent leather with Laplacian Operator following with Gaussian filter.

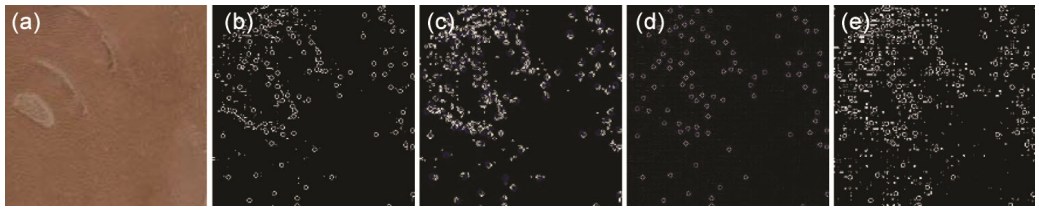

Fig. 6 — (a) Sample No 189 of actual intermittent leather, (b) Sample No 189 of actual intermittent leather with Gaussian filter, (c) Sample No 189 of actual intermittent leather with Laplacian Operator, (d) Sample No 189 of actual intermittent leather with Gaussian filter following with Laplacian Operator, and (e). Sample No 189 of actual intermittent leather with Laplacian Operator following with Gaussian filter.

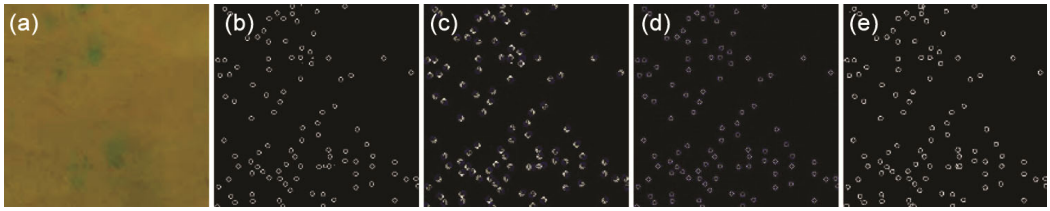

Fig. 7 — (a) Sample No 240 of actual intermittent leather, (b) Sample No 240 of actual intermittent leather with Gaussian filter, (c) Sample No 240 of actual intermittent leather with Laplacian Operator, (d) Sample No 240 of actual intermittent leather with Gaussian filter following with Laplacian Operator, and (e) Sample No 240 of actual intermittent leather with Laplacian Operator following with Gaussian filter.

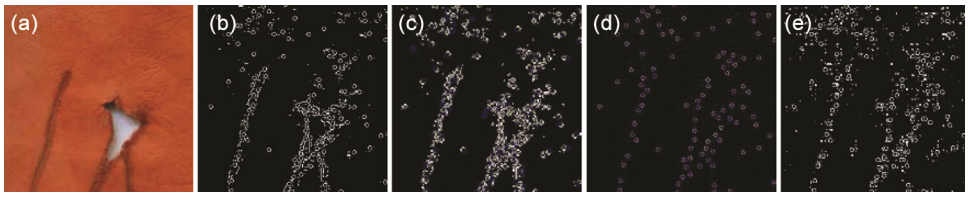

Fig. 8 — (a) Sample No 267 of actual intermittent leather, (b) Sample No 267 of actual intermittent leather with Gaussian filter, (c) Sample No 267 of actual intermittent leather with Laplacian Operator, (d) Sample No 267 of actual intermittent leather with Gaussian filter following with Laplacian Operator, and (e) Sample No 267 of actual intermittent leather with Laplacian Operator following with Gaussian filter.

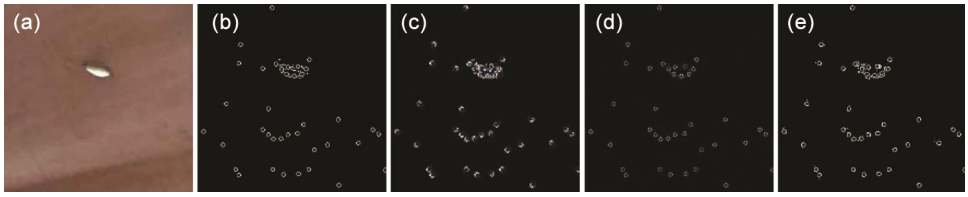

Fig. 9 — (a) Sample No 283 of actual intermittent leather, (b) Sample No 283 of actual intermittent leather with Gaussian filter, (c) Sample No 283 of actual intermittent leather with Laplacian Operator, (d) Sample No 283 of actual intermittent leather with Gaussian filter following with Laplacian Operator, and (e) Sample No 283 of actual intermittent leather with Laplacian Operator following with Gaussian filter.

features otherwise referred as statistical measures and this approach has been used in a number of applications. The feature represents the relationship of reference pixel (i) and neighboring pixel (j) in the angle 0. Each elements value has obtained as per the co-occurrence of pixels. The extracted GLCM features such as Contrast Eq. (4) is to measure the pixel intensity between a pixel and its neighbour in the whole image. Dissimilarity Eq. (5) is a measure to determine the distance between pairs of pixels in the region of interest. Homogeneity Eq. (6) is to measure the closeness of the distribution, Energy Eq. (7), is referred as steadiness in intensity of the pixel. Correlation Eq. (8) is a measure to understand the relationship among the pixels. Finally, Angular Second Moment (ASM) Eq. (9) is referred as uniformity which measures the strength of closeness of distribution. Accordingly, about 1132 images is generated under training dataset and 404 images is generated under testing dataset based on features extracted from GLCM as Class A, B, C, D, E, and F.

$$\text{Contrast}=\sum i \sum j (i-j)^2 P_{ij} \quad \ldots (4)$$

$$\text{Dissimilarity}=\sum i \sum j |i-j|^2 P_{ij} \quad \ldots (5)$$

$$\text{Homogeneity}=\sum i \sum j \, P_{ij} / 1 + (ij)^2 \quad \ldots (6)$$

$$\text{Energy}=\sum i \sum j \, P_{ij}^2 \quad \ldots (7)$$

$$\text{Correlation}=\sum i \sum j \, P_{ij} - \mu_x \mu_x / \sigma_x \sigma_x \quad \ldots (8)$$

$$\text{ASM}=\sum_{i,j=0}^{N-1} P_{ij}^2 \quad \ldots (9)$$

The classifier SLIC that segments a group of pixels, which have similar characteristics based on the color with the threshold value. Local clustering of pixels in five-dimension space defined by lO, x, y Eq. (10) values of the CIELAB (Lin and Lin *et al.*)[25] colorspace and m, n in Eq. (11) are co-ordinates of the pixels, [lOxy] Eq. (12). SLIC generates superpixels using Eq. (13) by clustering pixels on their color similarity and proximity in the image plane. There are two ways in segmentation, Agglomeration and divisive respectively as brought together and split the group until separate. For N/K pixels with K as input,

$$d_{lOxy} = \sqrt{(lO_q - lO_p)^2 + (x_q - x_P)^2 + (y_q - y_p)^2} \quad \ldots (10)$$

$$d_{mn} = \sqrt{(m_q - m_p)^2 + (n_q - n_p)^2} \quad \ldots (11)$$

$$D_s = d_{lOxy} + (m/S) * d_{mn} \quad \ldots (12)$$

$$SP = \sqrt{N/K},\ K \Rightarrow C_k = [lO_k, x_k, y_k, m_k, n_k] \text{ with } k=[p,q] \ldots (13)$$

Colorspace of lO*m*n Eq. (14) is arrived based on the ellipsoid as per foreground saliency method.

$$CV_{lOxy}(q,r) = 4/3\pi * lO(q,r) * x(q,r) * y(q,r) \quad \ldots (14)$$

The classifier, Minimum Spanning Tree Clustering (MSTC), segments on the threshold value through a graph using Eq. (15) which is undirected for p objects with vertices of each edges connected, which is a subset, the sum of weights of all edges is small based on the distance of r and s.

$$MSTC=\sum_{p\{r,s\} \in T} d(r,s) \quad \ldots (15)$$

Accordingly, the authors have generated 32 features from GLCM, SLIC and MSTC consisting of three datasets respectively as 24, 4 and 4.

2.3 Feature Selection and Classification

This section explains, selecting of key features to construct a suitable model from the extracted features consisting of 32 features from four datasets. As per the expert's distribution of homogeneous of color is one of the major concerns while aligning the intermittent leathers (Georgieva *et al*., and Pereira *et al*.,)[5-9]. The Gradient Boosting (Zhang *et al*.)[26] is employed to find out the suitable key feature from the four datasets by evaluating the least to most important predictor among the six features where f0, f1, f2, f3, f4, f5 respectively referred as Contrast, Dissimilarity, Homogeneity, Energy, Correlation. Key feature derived from four datasets consisting of DGF, DLO, DGFLO, DLOGF are respectively shown in Fig. 10 (a, b, c & d).

The authors have introduced a new method to construct the Image Score pattern (ISP) from the derived Key feature as shown in Equation Eq. (16). The value of T is computed by summing of values of A_i to F_i has to have value of minimum of 3, and the value of Z is derived from the key feature as shown in from Figure 2. Where Z_j=1, if it is having value of most important which is 3,4,5,6 and Z_j=0, if it is having value of least important which is 0,1,2.

$$ISP = \sum_{i=1}^{k} T_i * Z_j \quad \ldots (16)$$

Support Vector Machine (SVM) (Xia *et al*., and Ahmad *et al*.)[27-28] separates hyperplane with maximum margins in N-dimensional space that classifies on data points and generates significant accuracy having less computation. Further, the performance measures have been implemented using the confusion matrix (Haghighi *et al*.)[29], the value of True Positive (T+), False Positive (F+), False Negative (F-) and True Negative (T-) have calculated to understand the performance of Correct Classification of Defects versus Correct Non-Defect Classification of intermittent leather images as shown as sample diagram of Confusion Matrix in Table 1.

Statistical measurements for Correct and in-correct classification of defect versus non-defect leather images for the measures such as Accuracy Eq. (17), Error rate (18), Recall Eq. (19), False Positive Rate Eq.(20), Specificity Eq. (21), Precision Eq. (22), and Prevalence Eq. (23) are performed.

Table 1 — Sample diagram of Confusion Matrix

Correct Classification of Defects	Misclassification of Non-Defect Classification
Misclassification of Defect	Correct Non-Defect Classification

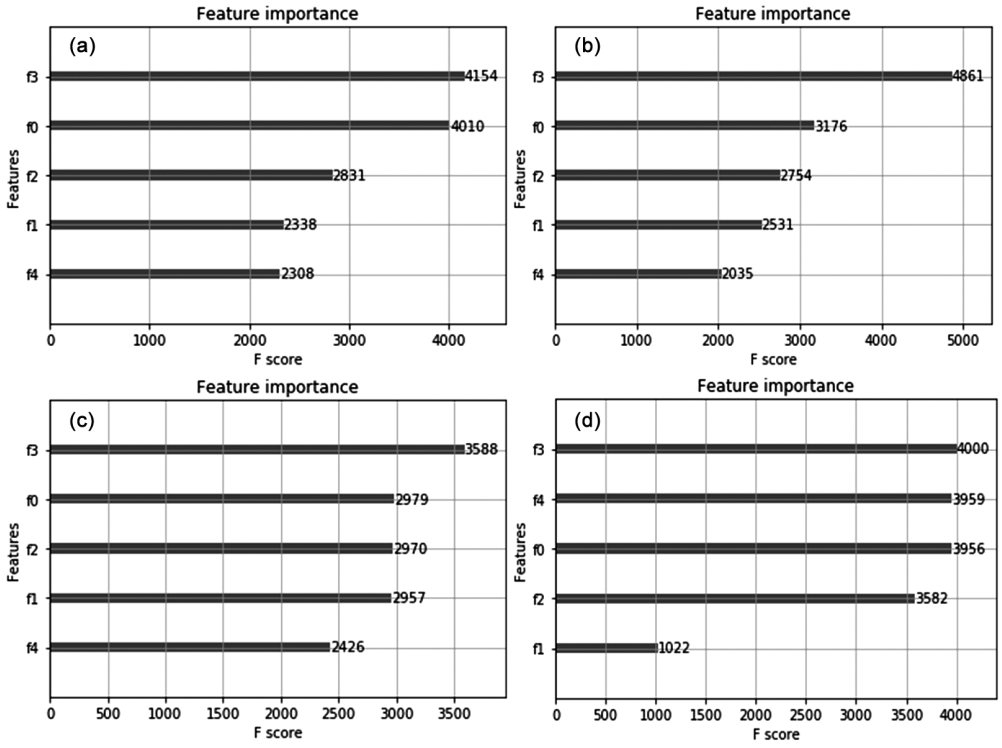

Fig. 10 — Least to Most Important Predictor of four datasets (a) DGF, (b) DLO, (c) DGFLO, & (d) DLOGF.

$$\text{Accuracy} = ((T+) + (T-)) / N \quad \ldots (17)$$

$$\text{Error Rate} = ((F+) + (F-)) / N \quad \ldots (18)$$

$$\text{Recall} = (T+) / ((T+) + (F-)) \quad \ldots (19)$$

$$\text{False Positive Rate} = (F+) / ((T-) + (F+)) \quad \ldots (20)$$

$$\text{Specificity (S)} = (T-) / ((T-) + (F+)) \quad \ldots (21)$$

$$\text{Precision (P)} = (T+) / ((T+) + (F+)) \quad \ldots (22)$$

$$\text{Prevalence} = ((T+) + (F-)) / N \quad \ldots (23)$$

3. Results and Discussion

The distribution of homogeneous pixels and non-homogeneous pixel for the pre-processed images using Gaussian filter, Laplacian Operator, Gaussian filter following with Laplacian Operator, Laplacian Operator following with Gaussian filter are examined for 384 by converting into 1536 images under the four image datasets namely DGF, DLO, DGFLO and DLOGF.

Based on the maximum importance of F-Score value the Key Feature key is energy as identified by having values maximum as DGF with 4154, DLO with 4861, DGFLO – f3 with 3588 and DLOGF – f3 with 4000. Accordingly, the value of Class label GL is generated. The algorithm to construct ISP is shown in Table 2.

The output values generated out of ISP are shown in the Table 3.

The class value of GLISP is 1 when the sum of value of features A to F is greater than intensity value

Table 2 — Filtering and Selection of the key feature

REQUIRE, Image Score Pattern (ISP),
GLISP is the Class Label, Sum of class lables A to F is T value to Count Area (CA) and value of D is 0.75, 0.54, 0.38 and 0.77

```
if T>= 3 and KF > D then
        Class GLISP= 1 {ie., Category – I}
Else
        Class GLISP= 2 {ie., Category – II}
end if
RETURN G {Class GLISP}
```

Table 3 — Image Score Pattern (ISP) Varieties

	A	B	C	D	E	F	T	GLISP
1	0	0	0	0	0	0	0	0
2	0	0	0	0	0	1	1	0
3	0	0	0	0	1	1	2	0
4	0	0	0	1	1	1	3	1
5	0	0	1	1	1	1	4	1
6	0	1	1	1	1	1	5	1
7	1	1	1	1	1	1	6	1
8	0	0	0	0	1	0	1	0
9	0	0	0	1	1	0	2	0
10	0	0	1	1	1	0	3	1
11	0	1	1	1	1	0	4	1
12	1	1	1	1	1	0	5	1
13	0	0	0	1	0	0	1	0
14	0	0	0	1	0	1	2	0
15	0	0	1	1	0	1	3	1
16	0	1	1	1	0	1	4	1
17	1	1	1	1	0	1	5	1
18	0	0	1	0	0	0	1	0
19	0	0	1	0	0	1	2	0
20	0	0	1	0	1	1	3	0
21	0	1	1	0	1	1	4	0
22	1	1	1	0	1	1	5	0
23	0	1	0	0	0	0	1	0
24	0	1	0	0	0	1	2	0
25	0	1	0	0	1	1	3	0
26	0	1	0	1	1	1	4	1
27	1	1	0	1	1	1	5	1
28	1	0	0	0	0	0	1	0
29	1	0	0	0	0	1	2	0
30	1	0	0	0	1	1	3	0
31	1	0	0	1	1	1	4	1
32	1	0	1	1	1	1	5	1

3 and the value of key feature is 1 and otherwise the class value of GLISP is 2. Accordingly, a new Class label GLISP is created. Further, Class label SL is having value as 81 and 82 for image Datasets DGF, DLO, DGFLO and DLOGF for taken for processing in binary as 0 and 1. Meanwhile from MSTC, the Class label M is noted the value as 18.35, 0.15, 0.05 and 45.97 in generated image Datasets such as DGF, DLO, DGFLO and DLOGF.

The Table 4 indicates the corresponding values of the sample images confirms the share of percentage of accuracy of the image datasets constructed based on Image Score Pattern is to the tune of 62.5%, 37.5%, 75% and 75 % respectively for DGF, DLO, DGFLO and DLOGF in classification of classification of defects and non-defects intermittent leather images.

The predicted value of confusion matrix is given in Table 5 of datasets consisting of GLCM, SLIC, MSTC and GLCM ISP. These confirms that the Correct Defect Classification of the dataset consisting of images with Laplacian Operator following with Gaussian filter of GLCM ISP is performing better than the other datasets as 103 and 40. However, interestingly it is noted that the in correct non-defect classification and a correct non-defect classification mong the datasets DLO and DGFLO of SLIC and MSTC is misleading. Similarly in the case of GLCM and GLCM ISP it is observed that dataset DLOGF is unique. These confirms the proposed GLCM ISP is significantly classifying.

The results of statistical measures as showed in Table 6 confirms the classification accuracy of DGF dataset of as 74% in GLCM, DGFLO dataset as 87% in SLIC, DLO dataset as 74% in MSTC and DLOGF dataset as 84% in proposed GLCM ISP. Interestingly it is observed that the proposed hybrid based approach to generate Datasets by combining together Gaussian filter and Laplacian Operator are performing significantly among the other datasets. Though the value of DGFLO of SLIC is higher than the DLOGF of GLCM-ISP, since the rate of incorrect non-defect classification and correct non-defect classification is high, the results of Dataset consisting of images with Laplacian Operator following with Gaussian filter (DLOGF) is significantly edging over the images with Gaussian filter following with Laplacian Operator (DGFLO).

Further, the other performance measure such as Error Rate, Recall, False Positive Rate, Specificity, Precision, and Prevalence are also confirming that among the datasets GLCM ISP is performing better for this datasets. The authors reporting that

Table 4 — Sample Image and its corresponding ISP value

Actual	DGF	DLO	DGFLO	DLOGF
(a)	(b)	(c)	(d)	(e)
3	T-2 and 0	T-3 and 1	T-3 and 0	T-2 and 0
17	T-2 and 0	T-2 and 0	T-3 and 0	T-2 and 0
29	T-4 and 1	T-4 and 1	T-5 and 1	T-2 and 0
84	T-4 and 1	T-3 and 1	T-4 and 1	T-4 and 1
189	T-4 and 1	T-3 and 1	T-4 and 1	T-4 and 1
240	T-3 and 0	T-2 and 0	T-4 and 1	T-2 and 0
267	T-4 and 1	T-3 and 1	T-4 and 1	T-4 and 1
283	T-3 and 0	T-2 and 0	T-2 and 0	T-2 and 0
Result	62.5 %	37.5 %	75%	75%

Table 5 — Predicted Values of datasets consisting of GLCM, SLIC, MSTC and GLCM ISP

	Correct Defect Classification				In-Correct Non-Defect Classification			
Feature / Dataset	DGF	DLO	DGFLO	DLOGF	DGF	DLO	DGFLO	DLOGF
GLCM	106	79	76	120	0	0	0	0
SLIC	83	0	0	65	0	61	19	0
MSTC	63	65	0	81	0	7	88	0
GLCM ISP	106	79	76	103	0	0	0	0
Feature / Dataset	In-Correct Defect Classification				Correct Non-Defect Classification			
	DGF	DLO	DGFLO	DLOGF	DGF	DLO	DGFLO	DLOGF
GLCM	37	63	53	23	0	1	14	0
SLIC	60	0	0	78	0	82	124	0
MSTC	80	30	0	47	0	41	55	15
GLCM ISP	37	63	53	40	0	1	14	0

Table 6 — Comparison of Statistical measurement

Metrics	Dataset	Accuracy	Error Rate	Recall	False Positive Rate	Specificity	Precision	Prevalence	Support
GLCM	DGF	0.74	0.26	0	0	1	0	0.26	143
	DLO	0.56	0.44	0.02	0	1	1	0.45	143
	DGFLO	0.63	0.37	0.21	0	1	1	0.47	143
	DLOGF	0.72	0.28	0	0	1	0	0.28	143
SLIC	DGF	0.58	0.42	0	0	1	0	0.42	143
	DLO	0.57	0.43	1	1	0	0.57	0.57	143
	DGFLO	0.87	0.13	1	1	0	0.87	0.87	143
	DLOGF	0.45	0.55	0	0	1	0	0.55	143
MSTC	DGF	0.44	0.56	0	0	1	0	0.56	143
	DLO	0.74	0.26	0.58	0.1	0.9	0.85	0.5	143
	DGFLO	0.38	0.62	1	1	0	0.38	0.38	143
	DLOGF	0.67	0.33	0.24	0	1	1	0.43	143
GLCM - ISP	DGF	0.74	0.26	0	0	1	0	0.26	143
	DLO	0.56	0.44	0.02	0	1	1	0.45	143
	DGFLO	0.63	0.37	0.21	0	1	1	0.47	143
	DLOGF	0.84	0.16	0	0	1	0	0.16	143

Table 7 — Comparison of SVM Score

Model suggested by	Technique	No. of Images	Accuracy
Patricio Villar, *et al.*[8]	Local binary Patterns and Gabor Features	1769	95%
Shivashankar S *et al.*[9]	Intensity of color and K-Nearest Neighbour (K-NN)	164	89.47%
Pereira, R.F. *et al.*[10]	Gray Level Co-occurrence Matrix (GLCM), Local Binary Patterns (LBP) and Structural Co-occurrence Matrix (SCM) and Classifer: K Nearest Neighbors (KNN), Multi Layer Perceptron (MLP) and Support Vector Machine (SVM)	1874	86%
Jawahar, M, *et al.*[11]	Multi-level thresholding algorithm and AI	90	88.6%
Sze-Teng Lion, *et al.*[12]	segment irregular regions and deep learning model	584	91.5%
Amorim, W.P. *et al.*[14]	Five discriminant analysis consisting of FisherFace, CLDA, DLDA, YLDA and KLDA	2000	90.3% for Wet-blue and 92.23% for Raw-hide
Authors of this Paper	Gaussian filter and Discrete Wavelet Transform, Gray Level Co-occurrence Matrix, Proposed Image Score Pattern, and Support Vector Machine	384	84%

this proposed approach as shown in Table 7 is better in assist the assorts as an extended facility while the aligning of intermittent leather.

3 Conclusion

The authors have proposed in aligning similar intermitted leather images based on Image Score Model derived from key feature obtained using gradient boosting and area of usefulness using new algorithm. Training and Testing dataset of intermittent leather images are generated based on features extracted about 384 and 144 respectively of Gray Level Co-occurrence Matrix, Simple Linear Iterative Clustering and Minimum Spanning Tree Clustering. The results are obtained with the classifier, Support Vector Machine for evaluation of the. The results of the classifier SVM for this dataset confirms that GLCM extracted features are faultless with the accuracy of 84%. Whereas, the other performance measures such as Accuracy, Precision, Recall, Specificity and Error Rate are also confirming that the proposed method can give supportive assistance to the assorts for aligning of intermittent leather. In the future work, the study of intermittent leather may be focused on species wise aligning pertaining to Bovine and Ovine.

Acknowledgement

The authors are thankful to Department Computer Science, University of Madras, Chennai, India and CSIR-Central Leather Research Institute (CSIR-CLRI), Chennai, India. The authors would like to sincerely acknowledging the support extended from Tanners Association. The authors also acknowledge the CSIR-CLRI Communication No. 1335.

References

1 Mascianà P, *World statistical compendium for raw hides and skins, leather and leather footwear*, (2015).
2 http://leatherindia.org/industry-at-a-glance (11 May 2019).
3 Vasagam S, Madhan B, Chandrasekaran B and Rao J R, *J Am Leather Chem Assoc*, 108 (2013) 210.
4 Poelzleitner, W &Niel A, *In Machine Vision Applications, Architectures, and Systems Integration,* 2347 (1994) 50.
5 Georgieva, L, Krastev, K and Angelov, N, *In CompSys Tech*, 3 (2003) 303.
6 Viana Roberto, Ricardo B Rodrigues, Marco A Alvarez, and Hemerson Pistori, *In Pacific-Rim symposium on image and video Technology* (Springer, Berlin, Heidelberg), (2007).
7 Villar P, Mora M, Gonzalez P, *Lecture Notes in Computer Science*, (Springer, Berlin, Heidelberg), (2011).
8 Shivashankar S and Madhuri R Kagale, *Int J Comput Appl*, 180 (2018) 34.
9 Pereira, R F, Medeiros, C M and Rebouças Filho, P P, *International Joint Conference on Neural Networks,* (IEEE), (2018).
10 Jawahar, M and Vani, K, *J.Am Leather Chem Assoc*, 114 (2019).
11 Liong, Sze-Teng, ArXiv abs/1903.12139 (2019).
12 Aslam, M, Khan, T M, Naqvi, S S, Holmes, G and Naffa, R, *IEEE Access*, 7 (2019) 176065.
13 Amorim, W P, Pistori, H, Pereira, M C and Jacinto, M A C, *IEEE,* (2010) 353.
14 Baxes, G A, *Digital Image Processing Principles and Applications*, (Wiley), (2005).
15 Ekstrom M P, *Digital Image Processing Techniques*, (Academic Press), (2012).
16 Yang X, Teng G, Zhao H, Li G, An P and Wang G, *International Conference on Signal Processing, Communications and Computing,* (IEEE), (2014).
17 Wang X and Bu J, *Digital Signal Processing,* 20 (2010) 1173.
18 Sivakumar R, Gayathri M and Nedumaran D, *Conference on Open Systems*, (IEEE), 2010.
19 Hsu C and Wu J, *Analog and Digital Signal Processing*, 45 (1998) 1097.
20 Basu M, *IEEE Tran. Syst Man Cybern, Part C (Applications and Reviews),* 32 (2002) 252.
21 Bao P, Zhang L, and Wu X, *IEEE Trans Pattern Anal Mach Intell*, 27 (2005) 1485.
22 Wang X, *IEEE Trans Pattern Anal Mach Intell,* 29 (2007) 886.
23 Taneja A, Ranjan P and Ujjlayan, *International Conference on Reliability, Infocom Technologies and Optimization,* (IEEE), (2015).
24 Patel J M and Gamit N C*, International Conference on Wireless Communications, Signal Processing and Networking,* (IEEE), 2016.
25 Lin P T, and Lin B R, *IEEE/ASME International Conference on Mechatronic and Embedded Systems and Applications,* (IEEE), 2016.
26 Zhang F, Du B and Zhang L, *IEEE Trans Geosci Remote Sens,* 54 (2015) 1793.
27 Xia L, Meng J, Xu R, Yan B and Guo Y, *IEEE Microw Wirel Compon*, (2006).
28 Ahmad I, Basheri M, Iqbal M J and Rahim, *IEEE Access,* 6 (2018) 33789.
29 Haghighi S, Jasemi M, Hessabi S and Zolanvari A, *J Open Source Softw,* 3 (2018) 729.